

See discussions, stats, and author profiles for this publication at: <https://www.researchgate.net/publication/11291260>

Solvation Phenomena of a Tetrapeptide in Water/Trifluoroethanol and Water/Ethanol Mixtures: A Diffusion NMR, Intermolecular NOE, and Molecular Dynamics Study

ARTICLE *in* JOURNAL OF THE AMERICAN CHEMICAL SOCIETY · AUGUST 2002

Impact Factor: 12.11 · DOI: 10.1021/ja0259335 · Source: PubMed

CITATIONS

122

READS

70

4 AUTHORS, INCLUDING:



Marco Fioroni

46 PUBLICATIONS 951 CITATIONS

SEE PROFILE



Stefan Berger

University of Leipzig

289 PUBLICATIONS 4,659 CITATIONS

SEE PROFILE

Solvation Phenomena of a Tetrapeptide in Water/Trifluoroethanol and Water/Ethanol Mixtures: A Diffusion NMR, Intermolecular NOE, and Molecular Dynamics Study

M. Fioroni,[†] M. D. Diaz,[‡] K. Burger,[†] and S. Berger^{*,‡}

Contribution from the Institut für Organische Chemie, Universität Leipzig, Johannisallee 29, D-04103, Leipzig, Germany, and Institut für Analytische Chemie, Universität Leipzig, Linnéstrasse 3, D-04103 Leipzig, Germany

Received February 14, 2002

Abstract: Solvation of a tetrapeptide, NAc-Ser-Phe-Val-Gly-OMe (**1**), in water and in water/alcohol mixtures with 2,2,2-trifluoroethanol (TFE)/water or ethanol (ETH)/water has been studied by diffusion NMR and intermolecular NOE measurements. The experimental results were compared with those obtained from detailed Molecular Dynamics (MD) calculations. Independently, all three methods revealed preferential solvation on the surface of the peptide by TFE in the water/TFE mixtures, but not by ETH in the water/ETH mixtures. The MD calculations show that the TFE concentration coating the peptide is higher than that in the bulk, while for ethanol, the concentration is nearly equal to that in the bulk. Calculated site-specific preferential solvation data between TFE, ETH, and water with the different peptide groups have been compared with the NMR data and shown to be in general agreement with the experimental facts.

Introduction

Understanding the conformation of peptides and proteins from the simple structure of small peptides to the complex 3D folding of large proteins is fundamental for the research on the function of living systems. Currently, one tries to predict protein folding from a defined starting primary amino acid sequence and a well-defined environment,¹ because the folding process is a complex interaction between the environment and the amino acid sequence constituting the protein. Although numerous papers, both experimental and theoretical, have been devoted to these problems, until now the prediction of the final folded structure is not yet possible unequivocally. Short peptides which are able to form stable secondary structures can be experimentally more easily analyzed and are helpful models for the understanding of the folding process. With the Molecular Dynamics (MD) technique, reversible folding of different peptides has been described in the time scale of microseconds.^{2–11}

Of the different environmental parameters able to influence the folding of peptides, the solvent is one of the most important. In biological systems, water is the common solvent and protein studies are mainly conducted in this environment. Nevertheless, many proteins or peptides interact with the lipid bilayer. Some binary systems such as water/alcohol mixtures can represent a possible model to reproduce the hydrophobic/hydrophilic character of the membrane surface. For this reason, the effects of alcohols on proteins and peptides have been widely analyzed over the last few decades. Changing the physicochemical properties of the solvents can give fundamental insight into the thermodynamics and kinetics of the folding.^{12–14}

TFE (2,2,2-trifluoroethanol) is often used in peptide and protein structure studies, due to its ability to induce secondary structure transitions and to denature the native conformation of proteins.¹⁵ Compared with other alcohols such as methanol, ethanol (ETH), or *tert*-butyl alcohol, TFE shows some peculiar characteristics. At first, TFE is able to stabilize α -helices with intrinsic helical propensity, and can induce α to β transitions or vice versa.^{16,17} In addition, it is able to induce β -sheets, β -hairpins, and β -turns and to disrupt tertiary structures in proteins, preserving the secondary structures.^{18,19} Recently, new experimental and theoretical data point to the clusterization properties of TFE in the presence of water as the primary reason for the TFE effect. In the work of Hong et al.,²⁰ small-angle

* Corresponding author. E-mail: stberger@rz.uni-leipzig.de. Phone: +49 341 9736101. Fax: +49 341 9711833.

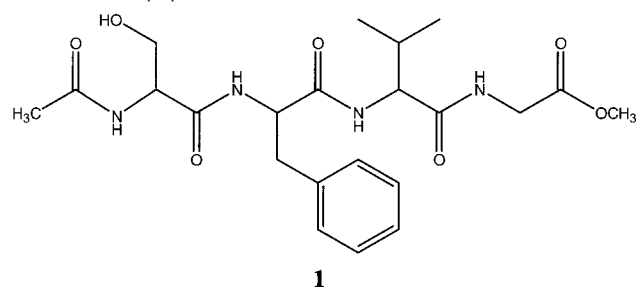
[†] Institut für Organische Chemie.

[‡] Institut für Analytische Chemie.

- (1) Pande, V. S.; Grosberg, A. Y.; Tanaka, T. *Rev. Mod. Phys.* **2000**, *72*, 259–314.
- (2) Shakhnovich, E. I. *Curr. Opin. Struct. Biol.* **1997**, *7*, 29–40.
- (3) Lazaridis, T.; Karplus, M. *Science* **1997**, *278*, 1928–1931.
- (4) Karplus, M.; Sali, A. *Curr. Opin. Struct. Biol.* **1995**, *5*, 58–73.
- (5) Ladurner, A. G.; Itzhaki, L. S.; Daggett, V.; Fersht, A. R. *Proc. Natl. Acad. Sci. U.S.A.* **1998**, *95*, 8473–8478.
- (6) Zhou, Y.; Karplus, M. *Proc. Natl. Acad. Sci. U.S.A.* **1997**, *94*, 14429–14432.
- (7) Duan, Y.; Kollman, P. A. *Science* **1998**, *282*, 740–744.
- (8) Daura, X.; Jaun, B.; Seebach, D.; van Gunsteren, W. F.; Mark, A. E. *J. Mol. Biol.* **1998**, *280*, 925–932.
- (9) Griffiths-Jones, S. R.; Searle, M. S. *J. Am. Chem. Soc.* **2000**, *122*, 8350–8356.
- (10) Blanco, F. J.; Serrano, L. *Eur. J. Biochem.* **1995**, *230*, 634–649.
- (11) Alvarado, R. M.; Blanco, F. J.; Serrano, L. *Nature Struct. Biol.* **1996**, *3*, 604–612.

- (12) Liu, Y. F.; Bolen, D. W. *Biochemistry* **1995**, *34*, 12884–12891.
- (13) Walgers, R.; Lee, T. C.; Cammers-Goodwin, A. *J. Am. Chem. Soc.* **1998**, *120*, 5073–5079.
- (14) Ionescu, R. M.; Matthews, C. R. *Nature Struct. Biol.* **1999**, *6*, 304–307.
- (15) Buck, M. *Rev. Biophys.* **1998**, *31*, 297–355.
- (16) Sonnichsen, S. P.; van Eyk, J. E.; Hodges, R. S.; Sykes, B. D. *Biochemistry* **1992**, *31*, 8790–8798.
- (17) Narhi, L. O.; Philo, J. S.; Li, T. S.; Zhang, M.; Samal, B.; Arakawa, T. *Biochemistry* **1996**, *35*, 11447–11453.
- (18) Luo, Y. Z.; Baldwin, R. L. *J. Mol. Biol.* **1998**, *279*, 49–57.
- (19) Reiersen, H.; Rees, A. R. *Protein Eng.* **2000**, *13*, 739–743.

Chart 1. Tetrapeptide 1



X-ray measurements of binary mixtures of methanol, ETH, TFE, and 1,1,1,3,3,3-hexafluoroisopropan-2-ol (HFIP) indicate strong clusterization of the fluorinated solvents, especially in the normally used 25–35% v/v range. These clusterization properties are directly related to the ability of these alcohols to induce strong secondary structure conformational changes.

Recently, some of us²¹ have experimentally demonstrated the preferential solvation of the tetrapeptide **1** by TFE in water mixtures using intermolecular NOE measurements. In a subsequent paper, we have also analyzed the solvation shell of the tetradecapeptide Bombesin²² with NOE studies, including detailed MD calculations. According to these MD calculations, the local concentration of TFE around the peptide is nearly 2 times higher than the nominal value of the bulk concentration (58% v/v compared to the starting bulk concentration of 30% v/v). The solvation shell properties around the peptides seem to be a necessary condition for the folding process in the presence of TFE. Interestingly, ethanol as the related alcohol of TFE, does not have the same folding induction properties. The replacement of the CH₃ group with the bulky and electron-withdrawing CF₃ group is responsible for the physicochemical properties and is important for the peptide–cosolvent interactions (i.e. acidity–basicity values of the OH group, free energy of hydration, dielectric constant). As proposed by Hong et al.,²⁰ the fundamental difference between the two cosolvents TFE and ETH is the lack of clusterization properties of ETH in water solutions. Therefore the properties of the solvation sphere coating the peptide in an aqueous mixture can be quite different between the two cosolvents. However, it is presently not decided whether clusterization and preferential solvation are intrinsically interconnected.

In this work, we report our findings on a comparison of the two solvent mixtures with respect of their solvation capability of a model tetrapeptide. We have analyzed the solvation shell properties of the model tetrapeptide in different water/TFE and water/ETH mixtures with experimental and MD methods. The peptide chosen contains aromatic and aliphatic side chains, the most simple amino acid glycine and an additional polar group in serine, thus it models on a very short path the most important amino acid features. The diffusion-NMR and intermolecular NOE measurements give basic information on the solvation shell characteristics. The experimental hydrodynamic radius is a sum of the peptide dimension itself and of the solvation sphere contribution. In our systems, the changes in the diffusion properties can be mainly correlated to the solvation sphere

properties in the different environments. Due to the smallness of the tetrapeptide used, no change of secondary structure in the two solvent systems is expected. In the unfolded state, the overall dimensions cannot vary too much to influence the diffusion measurements. In addition to the detection of global preferential solvation it was investigated whether some specific side chains of the peptide show a site-specific preferential solvation in the two cosolvents.

Parallel to the NMR analysis, a Molecular Dynamics study has been conducted. The TFE model developed in our group²³ is able to reproduce the activity coefficient of the water/TFE solutions in very good agreement with the experimental data.²⁴ This property is of fundamental importance concerning the cosolvent effects on peptides and proteins.²⁵ In this study, we used this model to analyze the solvation shell properties of the tetrapeptide comparing the theoretical with the experimental results. To analyze the peptide solvation shell for ethanol, a corresponding model²⁶ has been used. An analysis of preferential solvation on the overall surface of the peptide and of local preferential solvation at different side groups with different concentrations has been performed.

The reported results can be of importance for understanding the different folding properties induced on peptides and proteins by the TFE and ETH cosolvents in aqueous mixtures, elucidating the underlying mechanisms of the peptide–water–cosolvent interactions as a first step for the folding problem.

Experimental Section

General. The tetrapeptide NAc-Ser-Phe-Val-Gly-OMe was obtained as a gift from Professor K.-H. Röhm, University Marburg. Ethanol (HPLC grade) and TFE, deuterated ethanol, and deuterated water were purchased from Aldrich Chemical Co. and deuterated TFE from Cambridge Isotopes and used without further purification.

All binary mixtures were prepared volumetrically from these materials with deionized water obtained by passing it through a Modupore reverse osmosis purification system through a Moduplus ion exchange system. Peptide solutions were prepared by dissolution of the peptide in the appropriate water/alcohol mixture keeping the peptide concentration always constant at 0.043 M.

Viscosity Measurements. The viscosities (η) of water and/or alcohol (ETH, TFE) solutions with or without peptide were determined with an Ostwald viscometer. The temperature was monitored and controlled to ± 0.1 °C. As reference, the viscosity of protonated water at 25 °C was taken from the literature ($\eta_1 = 0.894$ cP) and correlated with the efflux time measured with a stopwatch (t_1). The viscosity of every solution (η_2) was calculated from its efflux time (t_2) and the corresponding efflux time of water (t_1) with the equation $\eta_1/\eta_2 = t_1/t_2$.

NMR Measurements. All NMR spectra were recorded on a Bruker DRX 400 spectrometer (9.4 T) at 298 K, using a 5 mm inverse probe equipped with z gradient coils capable of producing magnetic field pulse gradients in the z -direction of 56 G cm⁻¹.

DOSY NMR Spectra. A stimulated echo sequence incorporating bipolar gradients (BPPLIED²⁷) with a longitudinal eddy delay of 5 ms was used for acquiring DOSY spectra. Since no deuterated solvents were employed, the lock signal was adjusted to an external standard (capillary of d_6 -DMSO) contained in the 5 mm NMR tubes. The duration of the magnetic field pulse gradients (δ) and the diffusion times (Δ) were optimized for each sample to obtain complete dephasing

(20) Hong, D. P.; Hoshino, M.; Kuboi, R.; Goto, Y. *J. Am. Chem. Soc.* **1999**, *121*, 8427–8433.

(21) Diaz, M. D.; Berger, S. *Magn. Res. Chem.* **2001**, *39*, 369–379.

(22) Diaz, M. D.; Fioroni, M.; Burger, K.; Berger, S. *Chem.: Eur. J.* **2002**, *1663*–1669.

(23) Fioroni, M.; Burger, K.; Mark, A. E.; Roccatano, D. *J. Phys. Chem. B* **2000**, *104*, 12347–12354.

(24) Chitra, R.; Smith, P. E. *J. Chem. Phys.* **2001**, *115*, 5521–5530.

(25) Timasheff, S. N. *Adv. Protein Chem.* **1998**, *51*, 355–432.

(26) Müller-Plathe, F. *Mol. Simul.* **1996**, *18*, 133–143.

(27) Gibbs, S. J.; Johnson, C. S. *J. Magn. Reson.* **1999**, *93*, 395–402.

of the signals with the maximum gradient strength. Gradient strengths of 2.0–2.5 ms duration were incremented in 32 steps and the diffusion times were optimized for every experiment (typical values found for diffusion delay range from 50 and 85 ms for complete decay of the signals in binary mixtures and peptide solutions, respectively). The pulse gradients were incremented from 2% to 95% of the maximum gradient strength in a linear ramp and the data were recorded with 32 scans. An exponential window function with 1 Hz line broadening was applied before Fourier transformation.

NOE Experiments. Intermolecular NOE measurements in water/ETH and water/TFE mixtures were performed at 298 K on a Bruker DRX-400 spectrometer, using the modified DPGSE pulse sequence as described previously.²¹ For every ETH concentration, a series of 16 experiments with different mixing times (from 10 ms to 2.5 s) and with a relaxation delay of 2 s have been acquired. An exponential window function with 3 Hz line broadening was applied before the Fourier transformation and a baseline correction was conducted after the FT. The signals of interest were integrated and the integrals were scaled by a reference integral.

MD Methods. The starting structure of the tetrapeptide is the α -helix conformation. The N-terminus was acetylated and the C-terminus methylated. The peptide was then solvated in a cubic box with SPC water²⁸ and with two water mixtures of different concentrations for each TFE²³ and ETH²⁶ solvent model. The solvation process was performed by stacking equilibrated boxes of solvent molecules to form a box of 3.5 nm, large enough to contain the peptide and 1 nm of solvent on each side. All solvent molecules with atoms within 0.15 nm of the peptide have been removed. Since the protonation state of the peptide (at any pH) is 0, no counterions have been added to the simulation box. All MD simulations were performed by using an isothermal–isobaric ensemble through the Berendsen algorithm.²⁹ The temperature was kept constant at the reference value of 300 K by weak coupling to an external temperature bath with a coupling constant of 0.1 ps. The peptide and the rest of the system were coupled separately to the temperature bath. The LINCS³⁰ algorithm was used to constrain all bond lengths. For the water molecules, we used the SETTLE³¹ algorithm to constrain the bond lengths as well as the bond angles. A dielectric permittivity $\epsilon = 1$ for neat water and TFE/water mixtures has been used. For the ETH/water mixtures a reaction field was used, setting ϵ equal to 70 and 62 for the 16% v/v and 32% v/v, respectively. In all simulations a time step of 2 fs was used. The cutoff radius for the nonbonded interactions was set to 1.4 nm for the TFE/water mixtures simulations and 1.0 nm for the ETH/water boxes and the neat water.³² Different cutoff values and treatment of the electrostatic interactions were used, considering the different parametrization conditions of the cosolvent mixtures. An initial velocity obtained from a Maxwell distribution at the desired initial temperature has been assigned to all atoms. The density of the system was adjusted by performing the first equilibration runs at NpT conditions by weak coupling to a bath of constant pressure ($P_0 = 1$ bar, coupling time $\tau = 0.5$ ps, compressibility $\beta_T = 4.5 \times 10^{-5}$ bar⁻¹ for water and TFE/water mixture and 1.1×10^{-4} bar⁻¹ for ETH). All simulations were equilibrated for 100 ps for MD runs with position restraints on the peptide to allow relaxation of the solvent molecules. These first equilibration runs were then followed by other 100 ps runs without position restraints on the peptide. After equilibration the simulation time was 10 ns for all boxes. All MD runs and the analysis of the trajectories were performed with the GROMACS 2.0 software package³³ on a 1 GHz PC with a Pentium III processor.

Results and Discussion

Diffusion Measurements. Determination of self-diffusion coefficients in a multicomponent liquid system is a very helpful tool for extracting information about intermolecular interactions and the local structure of solutions. The diffusion coefficient of a single species can be converted into its hydrodynamic radius (also called the Stokes radius R_S) according to the Stokes–Einstein equation $R_S = k_B T / (6\pi\eta D)$, where k_B is the Boltzmann constant, T is the temperature (in K), and η is the viscosity of the solution. It has been observed that the experimental value is sometimes larger than the theoretical size of the single molecule under study. This result can be explained as a consequence of intermolecular interactions (e.g., intermolecular hydrogen bonding, aggregation) that increase the size of the “diffusion unit” which contains the molecule of interest and its surrounding, e.g., solvent or other solute molecules. In the particular case of peptides and proteins, diffusion measurements are useful for detecting aggregation phenomena. The enlargement of the size of the diffusion unit as a result of aggregation provides a proportional decrease of the diffusion coefficient. In addition, conformational interconversions of proteins also may be followed by concomitant changes observed in the diffusion coefficient.³⁴ As an example, the TFE-induced transition of a peptide from a larger random coil conformation to the more ordered α -helices was monitored by variations of the diffusion coefficient as a consequence of the reduction of its hydrodynamic radius. Thus, if neither aggregation nor conformational changes occur, the size of a peptide may be variable due to the interactions with the solvent present in solution.

To test the viability of our experimental method, we first measured the diffusion coefficients of water and alcohols of binary water/alcohol mixtures without peptide and compared these experimental values with those already published for water/ETH and water/TFE, respectively.³⁵ The satisfactory agreement between the published and our experimental results encouraged us to use the same procedure but with the peptide dissolved in these solutions. Two sets of peptide solutions in water/ETH and water/TFE at identical peptide but varying water/alcohol ratios have been prepared. In Figure 1a,b the diffusion coefficients of water, alcohol, and peptide are plotted versus the percentage of alcohol content. The diffusion coefficients of the peptide exhibit in both cases a similar behavior on the whole range of alcohol concentration: decreasing when the alcohol content increases and practically constant at an alcohol concentration higher than 30% v/v.

To estimate the hydrodynamic radius of any species from its diffusion coefficient value, one has to determine the viscosity of the solution. Therefore, we measured the viscosities of the two binary mixtures with and without peptide. Once again, the comparison of our experimental viscosity values with the data from the literature showed good agreement and validated the method. The results of the viscosity measurements of the peptide solutions are given in Tables 1 and 2. If one compares the viscosity of solutions with and without peptide, no substantial

(28) Berendsen, H. J. C.; Grigera, J. R.; Straatsma, T. P. *J. Chem. Phys.* **1987**, *91*, 6269–6271.

(29) Berendsen, H. J. C.; Postma, J. P. M.; DiNola, A.; Haak, J. *J. Chem. Phys.* **1984**, *81*, 3684–3690.

(30) Hess, B.; Bekker, H.; Berendsen, H. J. C.; Fraaije, J. G. E. M. *J. Comput. Chem.* **1997**, *18*, 1463–1472.

(31) Miyamoto, S.; Kollman, P. A. *J. Comput. Chem.* **1992**, *13*, 952–962.

(32) van der Spoel, D.; van Maaren, P. J.; Berendsen, H. J. C. *J. Chem. Phys.* **1998**, *108*, 10220–10230.

(33) van der Spoel, D.; Berendsen, H. J. C.; van Buuren, A. L.; Apol, E.; Meulenhoff, P. J.; Sijbers, A. M. T. L.; Van Drunen, R. GROMACS User Manual, 1995 (<http://www.gromacs.org>).

(34) Rogers-Sanders, S. A.; Vander Velde, D.; Larive, C. K. *Fresenius J. Anal. Chem.* **2001**, *369*, 308–312.

(35) Harris, K. R.; Newitt, P. J.; Derlacki, Z. J. *J. Chem. Soc., Faraday Trans.* **1998**, *94*, 1963–1970.

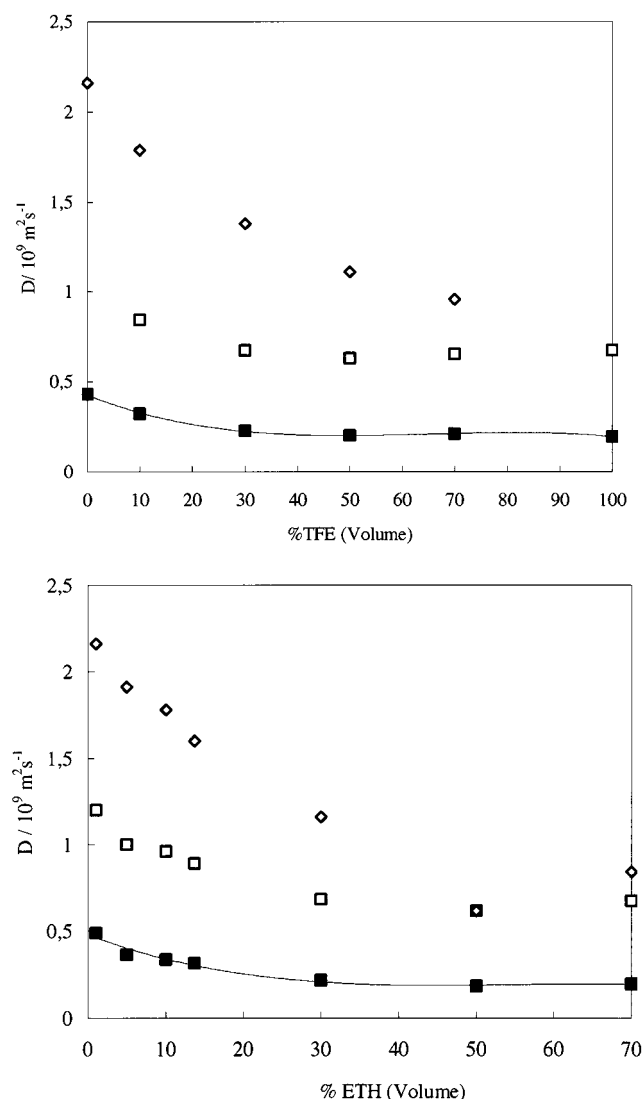


Figure 1. (a) Diffusion coefficients at 25 °C of water (\diamond), TFE (\square), and peptide (\blacksquare) in water/TFE/peptide solutions as a function of TFE concentration. (b) Diffusion coefficients at 25 °C of water (\diamond), ETH (\square), and peptide (\blacksquare) in water/ETH/peptide solutions as a function of ETH concentration.

Table 1. Viscosities (η) for Water–TFE and Water–TFE–Peptide at 25 °C

% vol (TFE)	$\eta_{\text{TFE}}^{\text{water-TFE}}/\text{cP}$	$\eta_{\text{water-TFE-peptide}}/\text{cP}$
0	0.894 \pm 0.011	0.942 \pm 0.016
1	0.94 \pm 0.09	0.968 \pm 0.024
5	0.977 \pm 0.014	1.037 \pm 0.017
10	1.06 \pm 0.019	1.169 \pm 0.019
30	1.376 \pm 0.022	1.447 \pm 0.024
50	1.472 \pm 0.026	1.641 \pm 0.031
70	1.407 \pm 0.025	1.502 \pm 0.031
100	1.23 \pm 0.032	1.35 \pm 0.033

deviations are observed in the case of ETH as cosolvent but a significant variation of the viscosity occurs when the peptide is present in TFE mixtures. This might be interpreted as an indication of the special properties of water/TFE mixtures.

Taking into account the viscosities of the samples, we finally calculated the hydrodynamic radius of the peptide from the Stokes–Einstein equation given above. These variations of the hydrodynamic radius are shown in Figure 2 as a function of the alcohol concentration for both ETH and TFE solutions.

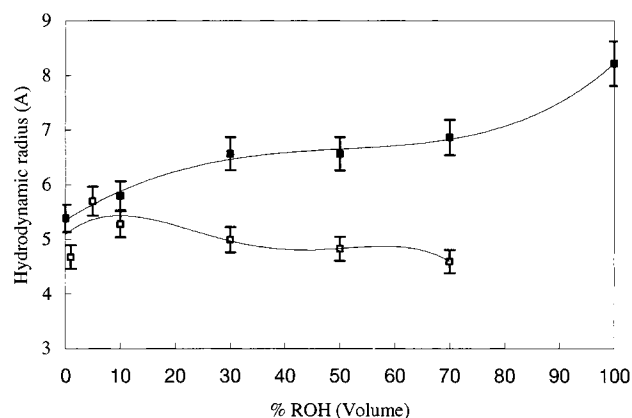


Figure 2. Comparison of the hydrodynamic radius of peptide at 25 °C in water/TFE/peptide (\blacksquare) and water/ETH/peptide (\square) solutions as a function of alcohol concentration.

Table 2. Viscosities (η) for Water–ETH and Water–ETH–Peptide at 25 °C

% vol (ETH)	$\eta_{\text{water-ETH}}/\text{cP}$	$\eta_{\text{water-ETH-peptide}}/\text{cP}$
0	0.894 \pm 0.011	0.942 \pm 0.016
1	0.896 \pm 0.014	0.952 \pm 0.016
5	1.026 \pm 0.01	1.055 \pm 0.019
10	1.174 \pm 0.017	1.227 \pm 0.017
30	1.964 \pm 0.019	2.009 \pm 0.038
50	2.439 \pm 0.024	2.477 \pm 0.036
70	2.335 \pm 0.027	2.429 \pm 0.039
100	1.348 \pm 0.018	

From the inspection of Figure 2 one can see that in the TFE solutions the size of the peptide exhibits an overall tendency to increase with the alcohol concentration, whereas in the ETH mixtures it remains practically constant, if not smaller, than in pure water. At high TFE concentrations (> 10% TFE) the peptide becomes much larger than in water or in water/ETH. In light of the MD calculations described below, we interpret these findings as a preferential coating of the TFE molecules in the water/TFE solutions which cover effectively the surface of the peptide increasing its “apparent size”.

Intermolecular NOE Measurements. In the course of our investigations about the TFE effect on peptides, we have previously studied both water/peptide and TFE/peptide interactions by detection of intermolecular homo- and heteronuclear NOEs, respectively. Since we compare here the solvent systems TFE/water and ETH/water, we present our experimental results of homonuclear NOEs in ETH/water solutions. We prepared a set of NMR samples with identical peptide concentration and volume ratio (1, 5, 10, 30, 50, and 70% volume of ETH as we reported previously for water/TFE). Identical NOE experiments under the same experimental conditions were performed.²¹ Chemical shift and multiplicity of the signals are very similar when compared with water/TFE solutions and the assignment was achieved by using standard 2D NMR methods. The intermolecular NOE’s in the water/peptide mixtures were measured by using the DPGSE-NOE sequence at different mixing times and integrating the signals of interest. In Figure 3 the NOE build-up curves are shown for a few representative groups, normalized to an equal number of protons.

The initial slope of the curves is different and this is experimental evidence of a differential interaction of water with the individual parts of the peptide. Applying the method of the

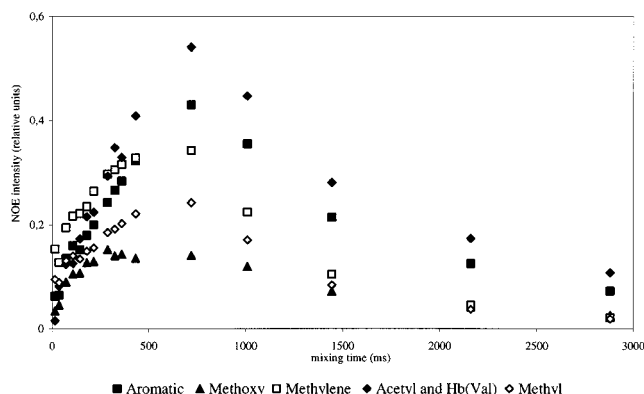


Figure 3. Experimental intermolecular homonuclear NOE enhancements between water and selected protons of tetrapeptide as a function of the mixing time in a 90% water/10% ETH mixture.

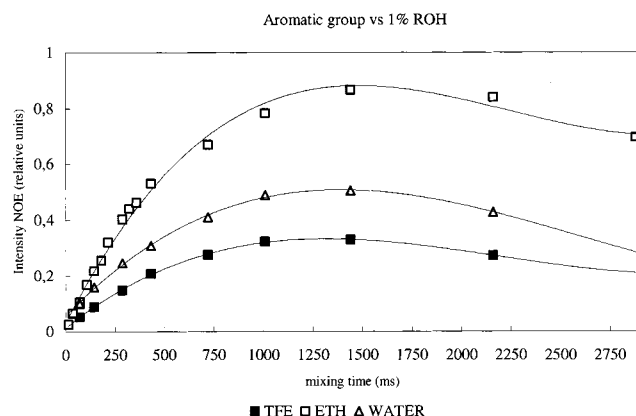


Figure 4. Experimental intermolecular homonuclear NOE enhancements between water and the aromatic side chain of the peptide in pure water, 1% ETH/water and 1% TFE/water as a function of the mixing time.

initial build-up rate, such site specific interactions between water and selected groups can be quantitatively evaluated and might be correlated with the vicinity of water molecules to the peptide surface. On the basis of the initial slope values, an order of solvation or water exposure has been established and shown to be independent from the ETH concentration: $\text{CH}_2(\text{Phe}) > \text{aromatic}(\text{Phe}) \approx \text{N-acetyl/Hb}(\text{Val}) \approx \text{Me}(\text{Val}) > \text{methoxy}$.

Surprisingly, the comparison of the NOE intensities at different ETH concentrations with the observed ones in pure water revealed an unexpected *increase* of the NOE intensities between water and almost all investigated proton sites when the ETH concentration is very low (1 or 5% ETH). This result demonstrates that water is “closer” to the peptide in ETH solutions than in pure water. This may be explained by changes in the internal and rigid structure of water when small amounts of ETH are added. An example of the effect is shown in Figure 4, where the intermolecular NOE between water and the aromatic side chain of the peptide in pure water, 1% of TFE, and 1% of ETH is given. Besides the already mentioned closeness of water to the peptide when ETH is present, the extraordinary difference of the NOE intensities between water and peptide in ETH and TFE is remarkable. The water/peptide contact diminishes dramatically in 1–10% TFE, until it almost disappears at TFE concentrations higher than 30%. In contrast, the presence of ETH does not substantially affect the water/peptide contacts, whereas at very low ETH concentration it helps to increase the water peptide contact.

Table 3. Composition of the Simulation Boxes^a

no. of SPC	no. of TFE	% v/v	x (mol fract)	R_g (nm)
879	0			0.44 ± 0.04
706	76	28	9.7×10^{-2}	0.43 ± 0.05
1631	76	14	4.4×10^{-2}	0.45 ± 0.04
no. of SPC	no. of ETH	% v/v	x (mol fract)	R_g (nm)
725	111	32	1.3×10^{-1}	0.42 ± 0.04
1775	111	16	5.9×10^{-2}	0.44 ± 0.05

^a No. of TFE, ETH, and SPC = number of trifluoroethanol (TFE), ethanol (ETH), and water (SPC) molecules, respectively; % v/v = volume percentage of the TFE and ETH cosolvents; x (mol fract) = molar fractions of the TFE and ETH cosolvents; R_g = calculated gyration radii of the peptide in the different solutions.

MD Analysis. In Table 3 the compositions of the different solvent boxes used in the simulations are summarized. The bulk concentrations in TFE are 28% v/v and 14% v/v, while the ETH mixtures are 32% v/v and 16% v/v, respectively. The molar volumes used for the TFE, ETH, and SPC models are 0.070, 0.058, and 0.019 L mol⁻¹, respectively.

The starting structure of the tetrapeptide was chosen to be an α -helix for all solutions. This has been done to test a possible different stability of this form in neat water and water–cosolvent mixtures. As expected, due to the small dimensions of the peptide, the unfolding is very rapid in all media. This has been checked through a root-mean-square deviation (RMSD) of the peptide backbone atoms. In the presence of water and in a mixture with TFE and ETH, the peptide unfolds rapidly in the first nanoseconds of simulation. In the following 9 ns, the peptide remains in the unfolded state. All these results are in agreement with the CD and NMR experimental data, reported above.

In the experimental stage, the attention has been focused on the different hydrodynamic radii of the peptide in the different solutions. This property is dependent on the peptide volume itself and the solvation shell around it. If the peptide is large enough to have different folded states, the overall geometric dimensions of the peptide will change and the resulting experimental hydrodynamic radius should be strongly influenced. To learn if this possibility exists for the analyzed tetrapeptide, a gyration radii analysis has been performed. From this, it is possible to study the overall dimensions of the peptide, depending on the conformational, without the contribution of the hydration sphere. For all simulations the gyration radius is nearly 0.44 nm, having little difference in the second decimal place, with the fluctuations being in the same range. This denotes little variation between the different possible conformational states. This result can be expected because of the small dimensions of the peptide, which cannot give large variations in the overall dimensions between the different possible unfolded states. To analyze the composition of the solvation sphere of the peptide, a density analysis of the two different cosolvents around the peptide has been performed at two different levels. The first one was performed by dividing the cubic box into 20 different parallel slides and time averaging the density values of the different groups (peptide, water, and cosolvent), looking through the main backbone axis of the peptide. This procedure gives an estimation of the different solvent densities around the overall peptide. The partial densities are reported in Figures 5 and 6 for the ETH/water and TFE/water mixtures, respectively.

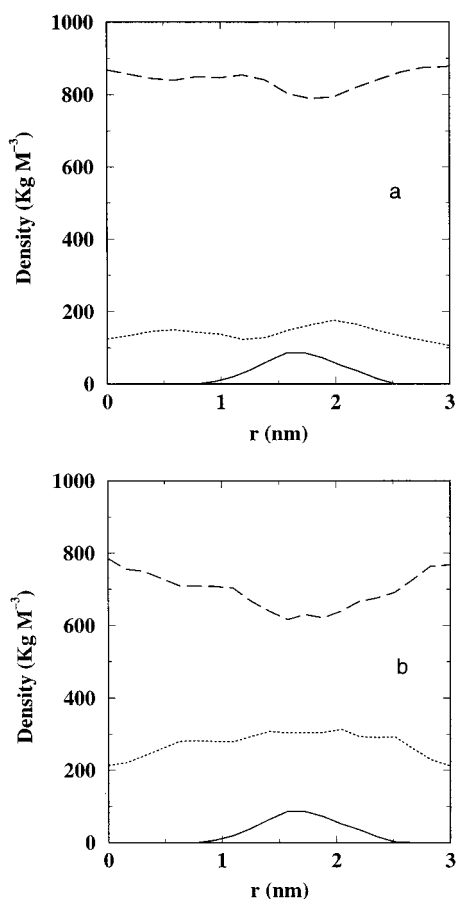


Figure 5. Density profiles (kg M^{-3}) of the different groups in the simulation box at 16% v/v ETH (a) and 32% v/v ETH (b). Long dashed line, water; dotted line, ETH; solid line, peptide.

In the ETH–water mixture with 16% v/v, the density of ETH around the peptide seems quite constant and close to the values of the bulk density. Only at 32% v/v is the local concentration of ETH somewhat higher than that of the bulk concentration at 0.09 kg L^{-1} . In the case of TFE and in both concentrations, the TFE around the peptide has a clearly higher density, if compared to the starting bulk. Observing the maximum density of TFE (600 and 310 kg m^{-3} in the 28% and 14% mixture) and the minimum water density (480 and 740 kg m^{-3}), it is possible to estimate the TFE concentration coating the peptide. In case of the 28% v/v of the bulk density in TFE, the concentration near the peptide is $\sim 46\%$ v/v while in case of the 14% v/v in TFE the coating density is 25% v/v. Obviously, the TFE molecules are able to create a coat around the peptide excluding water molecules. It should be underlined that previous calculations of the physicochemical properties of TFE/water mixtures report a system size independence^{23,24} from the box dimensions. Thus, the clusterization of TFE in water mixtures was not directly dependent from the size of the box.

While this analysis can be a first crude approximation of the phenomenon of the TFE coating, a second detailed study can be done by analyzing the local interactions between the cosolvents and the different peptide groups. In the NMR section, the intermolecular NOE intensities of the water, TFE, and ETH hydrogens with the peptide protons have been reported. The NOE intensities are practically absent for distances $>0.6 \text{ nm}$. To compare the experimental data with the simulation results, an analysis based on the number of contacts below a cutoff of

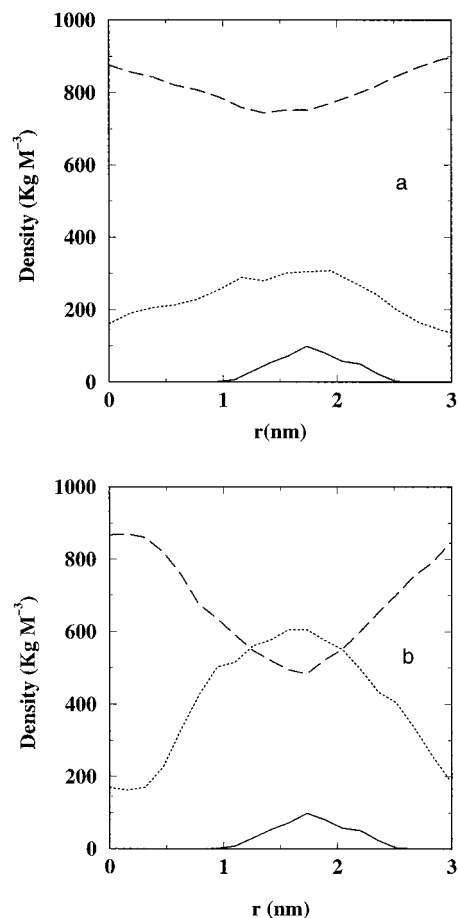


Figure 6. Density profiles (kg M^{-3}) of the different groups in the simulation box at 14% v/v TFE (a) and 28% v/v TFE (b). Long dashed line, water; dotted line, TFE; solid line, peptide.

0.6 nm and the average distance between different peptide–solvent groups has been performed. In Tables 4 and 5 the calculated distances and number of contacts of water and cosolvents with the different groups of the peptide are reported. The distances obtained from the simulation have been processed with use of the r^{-6} relationship.³⁶

In the case of TFE the distance and the number of contacts between the CH_2 group of TFE and the interesting groups of the peptide have been considered. The hydroxy groups of TFE and ETH have not been considered since the NOE data did not refer to this group (exchanging signal with water). At first glimpse, Table 4 shows that the contact numbers with ETH are directly proportional to the concentration (double contacts in the double concentrated solution), while in the TFE/water solutions this behavior is lost, due to the strong coat of TFE around the peptide. Considering the average number of contacts in a radius of 0.6 nm from a selected group, it is possible to calculate from the volumes excluded by the solvents the local concentration of the cosolvent. As reported in Table 4, the local concentration of TFE is higher than the starting bulk concentration around all groups and in both concentrations. In the case of the ETH/water solutions, ETH local concentration is lower than the bulk concentration for 32% v/v, while in the case of 16% v/v the concentration seems to be a little bit higher (2–8% v/v). In fact we have considered only molecules present in

(36) Tropp, J. J. *Chem. Phys.*, **1980**, 72, 6035–6043.

Table 4. Number of Contacts and Average Distances of TFE and Water (SPC) Molecules, Calculated for the Different Peptide Groups at Different TFE Concentrations^a

	dist (nm) of SPC	no. of contacts (<0.6 nm)	dist (nm) of TFE	no. of contacts (<0.6 nm)
CH ₂ (Phe)	0.30 ± 0.09	TFE = 28% v/v 4.3 ± 3.3	0.40 ± 0.06	1.8 ± 0.6 (71%)
aromatic(Phe)	0.31 ± 0.08	12 ± 9	0.36 ± 0.06	3.9 ± 1 (45%)
N-acetyl	0.35 ± 0.08	6.0 ± 4	0.41 ± 0.08	1 ± 0.5 (62%)
H _β (Val)	0.41 ± 0.08	10.2 ± 8	0.42 ± 0.06	3.35 ± 1.8 (55%)
Me(Val)	0.35 ± 0.08	3.6 ± 2.6	0.38 ± 0.06	1.1 ± 0.4 (53%)
CH ₂ (Phe)	0.30 ± 0.06	TFE = 14% v/v 6 ± 2.5	0.43 ± 0.06	1.2 ± 0.6 (43%)
aromatic(Phe)	0.29 ± 0.05	19 ± 9	0.39 ± 0.06	2.1 ± 0.9 (30%)
N-acetyl	0.31 ± 0.04	6.2 ± 2.5	0.45 ± 0.06	0.6 ± 0.4 (22%)
H _β (Val)	0.39 ± 0.06	12.2 ± 6.9	0.45 ± 0.06	2.8 ± 1.15 (46%)
Me(Val)	0.33 ± 0.06	4 ± 2	0.40 ± 0.06	1.0 ± 0.4 (48%)

^a Local concentrations of TFE in % v/v are reported in bold face.**Table 5.** Number of Contacts and Average Distances of ETH and Water (SPC) Molecules, Calculated for the Different Peptide Groups at Different ETH Concentrations^a

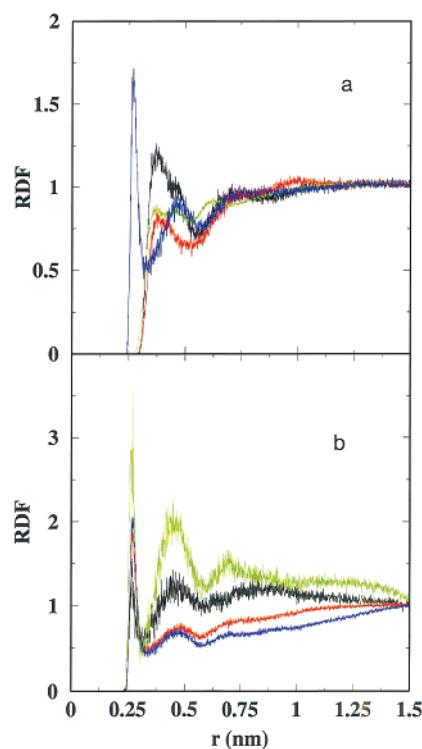
	dist (nm) of SPC	no. of contacts (<0.6 nm)	dist (nm) of ETH	no. of contacts (<0.6 nm)
CH ₂ (Phe)	0.30 ± 0.05	ETH = 32% v/v 9 ± 3	0.30 ± 0.05	2.44 ± 0.8 (30%)
aromatic(Phe)	0.28 ± 0.04	21.3 ± 6.2	0.26 ± 0.03	5.1 ± 1.67 (27%)
N-acetyl	0.36 ± 0.04	6.9 ± 2.1	0.33 ± 0.05	1.63 ± 0.7 (13%)
H _β (Val)	0.32 ± 0.03	27.4 ± 7.2	0.30 ± 0.05	4.9 ± 1.2 (22%)
Me(Val)	0.31 ± 0.04	7.1 ± 2.1	0.28 ± 0.03	1.83 ± 0.6 (28%)
CH ₂ (Phe)	0.30 ± 0.03	ETH = 16% v/v 13.5 ± 2.5	0.37 ± 0.1	1.14 ± 0.7 (18%)
aromatic(Phe)	0.26 ± 0.03	56 ± 6	0.31 ± 0.08	5.9 ± 1.7 (15%)
N-acetyl	0.34 ± 0.04	10.2 ± 2.1	0.37 ± 0.08	0.9 ± 0.5 (21%)
H _β (Val)	0.31 ± 0.03	37.4 ± 6.3	0.36 ± 0.11	2.67 ± 1.1 (18%)
Me(Val)	0.3 ± 0.03	8 ± 2	0.31 ± 0.08	0.9 ± 0.4 (26%)

^a Local concentrations of ETH in % v/v are reported in bold face.

a radius of 0.6 nm and, especially at low concentration of ETH, this may give poor statistics. In the TFE case, the central values of the local concentration around the groups are strongly deviating from the starting bulk concentration of the cosolvent, also including the strong fluctuations. From the NOE results of the water exposure the sequence CH₂(Phe) > aromatic(Phe) ≈ N-acetyl/H_β(Val) ≈ Me(Val) > methoxy was found. These results are mainly affected by the local concentration and distance between the groups considered. In Table 4 the calculated water distance from the analyzed groups follows quite well the experimental NOE sequence for both the TFE and ETH/water solutions. Distance and concentration fluctuations are high, and most probably longer simulation times will give better results, but the general trend seems to be confirmed with reasonable correlation between the experimental and theoretical results.

In addition, the structure of the solvation sphere for water, TFE, and ETH toward the different peptide groups has been analyzed through a radial distribution function (rdf) study. These data are highly important for understanding the hydrophobic hydration of proteins and biomolecules in general.^{25,37} Figures 7 and 8 show such curves.

The selected groups are the Ser oxygen (for the hydrogen bond interaction), the Phe CH₂ group and aromatic carbons, and the CH₃ groups of the Val residue. The last groups have been analyzed to note if there is any kind of different organization of water and cosolvents around the hydrophobic groups with aromatic or aliphatic character. In Figure 7a, the rdf water oxygen functions for the neat water solutions,

**Figure 7.** (a) Radial distribution function plot of the water oxygen and Ser oxygen (blue line), Val methyl groups (black), aromatic carbons (green), and methylene (red) group of the Phe residue (neat water). (b) rdf plot of the TFE (green), ETH (black), water in ETH mixture (red), and water in TFE mixture (blue) toward the Ser oxygen (28% v/v TFE, 32% v/v ETH).

surrounding the hydrophobic groups, and Ser are reported. The hydrogen bonding of the water with Ser is denoted by the sharp

(37) Meng, E. C.; Kollman, P. A. *J. Phys. Chem.* **1996**, *100*, 11460–11470.

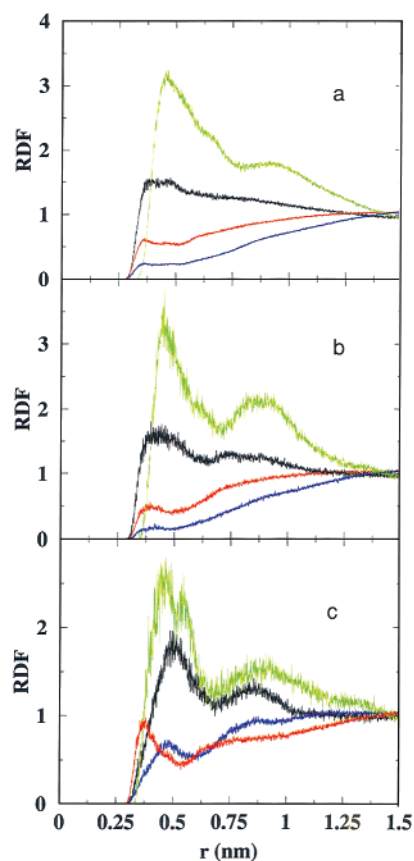


Figure 8. (a) Radial distribution function plot of the TFE central carbon (green), ETH central carbon (black), and water oxygens in TFE/water mixture (red) and ETH/water mixture (blue) with respect to the aromatic carbons of the Phe residue, (b) around the CH_2 groups of Phe, and (c) around the Val CH_3 groups (28% v/v TFE, 32% v/v ETH).

peak at 0.25 nm. The trend of the other curves is quite similar, denoting a typical “hydrophobic character”, with some differences between the aliphatic and aromatic solvation shells, as reported by Meng et al.^{37,38}

In Figure 7b, different rdf for the TFE and ETH/water solutions are reported. Water, TFE, and ETH interact with a hydrogen bond to Ser showing a sharp maximum at 0.25 nm. In the case of TFE a well-defined second and third peak are present, denoting a long-range organization of the solvation

sphere. Water and ETH also present a second peak denoting a lower long-range order if compared to TFE. In Figure 8a the rdf of water and cosolvents are reported for the Phe benzene ring. Compared to Figure 8b, where the rdf of the CH_2 group of Phe is reported, water, TFE, and ETH show a less organized structure. In the case of the CH_3 groups of Val (Figure 8c), the solvation shells of water and especially TFE and ETH show a long-range order, while for the CH_2 group of Phe, TFE seems to maintain the solvation structure in contrast to ETH and water. As a general phenomenon, the water structure is more organized in the presence of ETH compared to TFE, while TFE shows a long-range order higher than that found for ETH.

Conclusions

Diffusion NMR and NOE measurements have shown preferential solvation of a tetrapeptide by TFE. For better understanding of the dynamic processes involved in the experimentally detected solvation of the peptide, an additional MD study has been conducted. The preferential solvation of the peptide in the TFE/water mixtures compared to the corresponding ETH/water mixtures was confirmed. The relative density of TFE around the peptide deviates strongly from the average density found in the solution mixture. The same phenomenon has not been found for the ETH/water mixtures. The solvation shell around the peptide is mainly constituted by TFE molecules. This phenomenon explains the increase of the apparent hydrodynamic radius of the peptide, yielding an apparent increase of the dimensions that can perturb the diffusion properties. Site-specific intermolecular NOE effects can be reasonably modeled with the MD calculations. Although we are not yet able to decide whether the preferential solvation of the peptide by TFE results from a direct transfer of the peptide into a TFE cluster or is caused by a step by step coating with single TFE molecules, we can affirm that the TFE-solvating sphere of the peptide is very strong and stable. Further studies to elucidate the aforementioned problems are under investigation.

Acknowledgment. M. Dolores Díaz thanks the grant of fellowship (EX 99 25391200) by the Ministerio de Educación y Cultura of Spain. M. Fioroni thanks the TMR project “Fluorine: A Unique Tool for Engineering Molecular Properties” (ERBFMRXCT 970120). This work was funded by the Fonds der Chemischen Industrie.

(38) Linse, P. *J. Am. Chem. Soc.* **1990**, *112*, 1744–1748.